2022

The performance response of a heat pipe evacuated tube solar collector using MgO/MWCNT hybrid nanofluid as a working fluid

Ahmed A. Abdel-Rehim
ahmed.azim@bue.edu.eg

shady Henein

Case Studies in Thermal Engineering 33 (2022) 101957

Contents lists available at ScienceDirect

Case Studies in Thermal Engineering

journal homepage: www.elsevier.com/locate/csite

The performance response of a heat pipe evacuated tube solar collector using MgO/MWCNT hybrid nanofluid as a working fluid

Shady M. Henein [*], Ahmed A. Abdel-Rehim

The British University in Egypt, Department of Mechanical Engineering, Centre for Renewable Energy (CRE), Cairo, Egypt

A R T I C L E I N F O

Keywords:
Evacuated tube solar collector
Hybrid nanofluid
Solar energy
Thermal efficiency
Energy
Exergy

A B S T R A C T

Utilizing a hybrid nanofluid is a promising solution for enhancing the thermal performance of the solar collector in a sustainable manner. In the present work, the effect of using magnesium oxide/multi-walled carbon nanotubes (MgO/MWCNT) hybrid nanofluid on the thermal performance of the evacuated tube solar collector is experimentally investigated. Four different weight ratios of (80:20), (70:30), (60:40), and (50:50) are used for a hybrid of MgO with MWCNTs in a water base, respectively. The experiments are performed at a 0.02% particle concentration and at various volume flow rates ranging from 1 to 3 L/min. The results show an enhancement in the energy and exergy efficiencies with the increase in the weight ratios of MWCNTs nanoparticles and volume flow rate. The enhancement of the energy and exergy efficiencies of the collector is 55.83% and 77.14%, respectively, for MgO/MWCNT (50:50) hybrid nanofluid. It is found that increasing the weight ratio of MWCNTs nanoparticles from 20% to 30% achieves a significant increase in the collector efficiency enhancement compared to other hybrid nanofluids. The results conclude that MgO/MWCNT (50:50) performs better than all other hybrid nanofluids at all volume flow rates and is closer to MWCNT/water nanofluid.

1. Introduction

In recent years, the demand for enhancing the efficiency of solar thermal collectors has increased significantly. Without any external energy, solar thermal collectors convert the solar energy into heat energy that can be used for domestic and industrial applications [1]. The efficiency of the solar thermal collectors depends on the useful amount of heat obtained and transferred to the working fluid. Flat-plate solar collectors (FPSC) and Evacuated Tube solar collectors (ETSC) are the most common devices that are used in domestic applications, and their performance is influenced significantly by radiation, temperature, and working fluid [2].

Enhancing the thermophysical properties of the working fluid is an essential factor for improving the performance of solar applications such as parabolic trough collector [3], solar still [4], flat-plate solar collector [5] and evacuated tube solar collector [6]. Many studies have been conducted on adding nanoparticles to the working fluid to improve its thermal properties. Researchers are using nanofluid, which is a mixture of nanoparticles with a size less than 100 nm, with the base fluid to increase the thermal conductivity of the working fluid [7].

Raj and Subuddhi [8] highlighted the effect of using nanofluids on the performance of solar collectors. They demonstrated that the thermophysical properties of the working fluid were enhanced dramatically, and among different types of nanofluids, using Carbon nanotube (CNT) was found to have a great impact on the thermal performance of solar collectors. Sharafeldin et al. [9] investigated the

* Corresponding author.
E-mail address: Shady.magdy@bue.edu.eg (S.M. Henein).

https://doi.org/10.1016/j.csite.2022.101957
Received 3 February 2022; Received in revised form 16 March 2022; Accepted 18 March 2022
Available online 27 March 2022

Nomenclature

ETSC	Evacuated tube solar collector
MgO	Magnesium Oxide
MWCNT	Multi-walled carbon nanotube
A_c	Collector area (m^2)
C_p	Heat capacity (J/K)
T_a	Ambient Temperature (°C)
T_i	Fluid inlet temperature (°C)
T_o	Fluid outlet temperature (°C)
F_R	Heat removal factor
I_T	Radiation intensity (KW/m^2)
$\dot{m}$	Mass flow rate of the working fluid (Kg/s)
Q_u	Useful Energy Gain (W)
$\dot{S}_{gen}$	Entropy generation rate (J/K)
$\dot{Ex}_{dest}$	Exergy destruction rate (W)

Greek Symbols

α	Absorptivity
τ	Transmissivity
ε	Emissivity
ρ	Density (kg/m^3)
η	Energy Efficiency of the collector (%)
η_{ex}	Exergy Efficiency of the collector (%)
φ	Volume Fraction (%)

Subscripts

bf	Base fluid
nf	Nanofluid
np	Nanoparticles
hnf	Hybrid nanofluid

thermal performance of the ETSC using copper nanoparticles. The results concluded that increasing the volume concentration of the copper nanoparticles had enhanced the thermal performance significantly. The output temperature was increased by 50%, leading to a 34% area reduction in the solar collector. The energetic and exergetic efficiencies of ETSC were investigated in Ref. [10] using MWCNT/water nanofluid ranging from 0.005 to 0.05 (wt.%). The enhancements of the average energy and exergy efficiency of the ETSC were 55% and 10%, respectively.

Carbon-based nanoparticles have shown enhancement in the performance of solar applications. However, many challenges have been reported, such as the high cost of the raw material and poor rheological properties [11]. Researchers are still grappling with the challenges of using nanofluids in heat transfer devices. Therefore, addressing the drawbacks of nanofluids has made researchers invest in developing them by combining different nanoparticles in the base fluid known as "hybrid nanofluids." A single material can not provide excellent rheological and thermal properties simultaneously. Metal oxide nanoparticles have higher rheological properties than carbon-based nanoparticles. However, they have lower thermal properties. Compositing a mixture of two or more materials with different properties has dominated research in recent years due to its essential role in improving the heat transfer rate of solar applications [12].

The heat transfer characteristics of the hybrid nanofluids are enhanced compared to the unitary nanofluids. Studies were conducted in Ref. [13] to investigate the thermal properties of the hybrid nanofluids, and it was observed that the rate of heat transfer was higher in the case of hybrid nanofluids. Experiments were conducted in Ref. [14] to investigate the thermal conductivity of switched-walled carbon nanotubes (SWCNTs)/MgO-ethylene glycol hybrid nanofluid. The results showed that the thermal conductivity of the hybrid nanofluid was higher compared to the unitary nanofluids of SWCNTs and MgO.

An experimental analysis was conducted in Ref. [15] to investigate the effect of using MoS_2–Ag/H_2O hybrid nanofluid on the performance of a solar collector. The results revealed that increasing nanofluid concentration had enhanced the temperature difference of the inlet-outlet fluid by 4.93%. Studies were conducted in Ref. [16] to investigate the effect of using SiO_2/Cu hybrid nanofluid on the thermal performance of the U-tube solar collector. The results revealed that the thermal performance of the solar collector was enhanced significantly, and it was concluded that hybrid nanofluid had improved the heating capability of the working fluid by reducing the problem of precipitation. Abid et al. [17] conducted experiments to investigate the utilization of hybrid nanofluid in the ETSC integrated with four different cycles. The results revealed that using hybrid nanofluid enhances thermal performance by 10.42% compared to mono nanofluid. An experimental study was conducted in Ref. [18] to investigate the performance analysis of hybrid

Table 1
Specifications of the ETSC.

Specification	Dimension
Height	1975 mm
Width	1190 mm
Depth	135 mm
Gross Area	2.35 m^2
Aperture Area	1.407 m^2
No. of Evacuated Tube	15
Volume of the working fluid	3.46 L
Absorption efficiency	92%
Manifold Insulation Thermal conductivity	$K_i = 0.043$ W/m^2 K

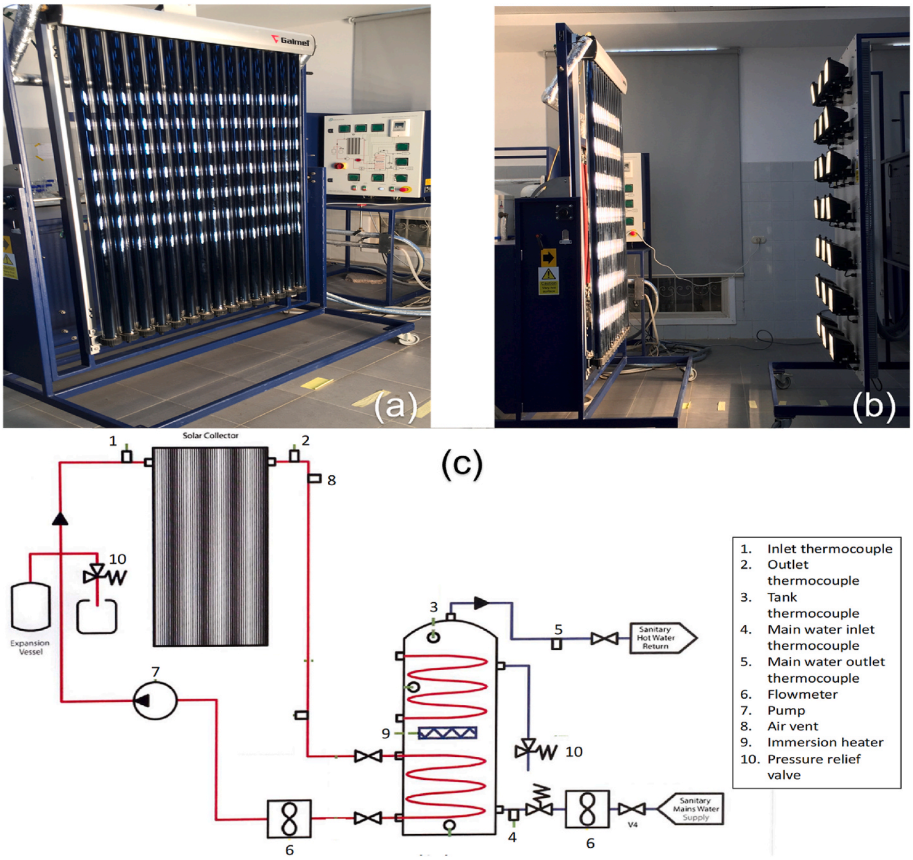

Fig. 1. (a) ETSC with control system (b) Artificial sunlight used in the experiment (c) Schematic diagram of the system.

nanofluids in FPSC. The author selected CuO and MgO hybrids with MWCNTs in a water base. The weight ratio of CuO/MWCNT and MgO/MWCNT hybrid nanofluid was (80:20). The results showed an improvement in the energy efficiency of the collector for MgO and CuO hybrid nanofluid of 70.55% and 69.11%, respectively.

As clearly stated in the literature review, hybrid nanofluids can achieve desirable results in solar collectors by selecting a suitable pair of nanomaterials. However, exploring the performance of hybrid nanofluids using different weight ratios for two nanomaterials has not been sufficiently investigated. Despite the poor rheological properties of carbon-based nanoparticles such as MWCNTs, they can enhance the thermal properties of metal oxide nanoparticles such as MgO by combining them in a fluid with appropriate ratios. The purpose of the current work is to experimentally investigate the potential of using MgO/MWCNT hybrid nanofluid with different weight ratios to enhance the thermal performance of the evacuated tube solar collector in terms of energy and exergy efficiencies.

2. Experimental setup

The present work was conducted to investigate the performance response of the ETSC by using different weight ratios of MgO/ MWCNT hybrid nanofluid in a water base at three different volume flow rates of 1 L/min, 2 L/min, and 3 L/min. The copper heat pipes in the ETSC transport the absorbed energy to the manifold to heat the working fluid. The working fluid flows to the heat exchanger coil that is inserted into a 210-liter tank, then it returns to the collector to close the cycle.

Table 1 presents the specifications of ETSC. Fig. (1.a) shows the setup of ETSC and control (on/off) valves used in the experiment to monitor the flow rate of the fluid, the inlet and outlet temperatures of the collector, and the temperature of the storage tank. Fig. (1.b) shows the artificial sunlight that stimulates the solar radiation to the collector. A Solar Power Meter sensor of model PYR 1307 was used to measure the radiation level, and it was controlled by a radiation controller of model 21 R7s 500-W. The ETSC and the storage tank inlet and outlet temperatures were measured by a thermocouple sensor of the model PT1000 type, while the flow rate of the working fluid was measured by a flow meter of the model YF-S201. Fig. (1.c) depicts a schematic diagram that describes all of the system's components.

2.1. Preparation and synthesis of hybrid nanofluid

In the present work, MWCNT/water, and MgO/water nanofluids were prepared at three different concentrations of 0.005, 0.01, and 0.02% using a two-step method. Hybrid nanofluid was prepared at the highest concentration at four different weight ratios of MgO/MWCNT (80:20), MgO/MWCNT (70:30), MgO/MWCNT (60:40), and MgO/MWCNT (50:50) in a water base. The first step is to prepare a solution of MgO/water at the highest concentration. The second step is to add the required quantity of MWCNTs to the solution and then sonicate it using an ultrasonic homogenizer type (UIP500hdT) having a frequency of 20 kHz for 7 h to produce the required weight ratios of the hybrid nanofluids.

3. Theoretical approach

In the present study, testing procedures of ASHRAE standard 93–2010 were performed, which imposed a record on each reading every 5 min to investigate the thermal performance of ETSC [10].

3.1. Energy calculations

The useful heat gain is calculated using the first law of thermodynamics as explained by Kalogirou [19],

$$Q_u = \dot{m} C_p \,(T_o - T_i) \tag{1}$$

Where $\dot{m}$ is the mass flow rate, Cp is the specific heat capacity of the working fluid, and To and Ti are the outlet and inlet temperatures of the collector, respectively. Another equation is presented to calculate the useful heat gain, which is given by

$$Q_u = A_c F_R [I_T\,(\tau\alpha) - U_L\,(T_i - T_a)] \tag{2}$$

Where F_R is the heat removal factor, and it represents the ratio of the actual heat energy gain to the maximum heat energy gained by the collector. A_c is the active area of the collector, I_T represents the solar irradiance, U_L is the overall heat loss coefficient of the collector, T_a is ambient temperature, τ and α represent the transmissivity of the glass and the absorptivity of the collector, respectively. The heat removal factor is represented by this equation

$$F_R = \frac{\dot{m} C_p \,(T_o - T_i)}{A_c F_R [I_T\,(\tau\alpha) - U_L\,(T_i - T_a)]} \tag{3}$$

The area of the collector is represented by this equation

$$A_c = \frac{\dot{m} C_p \,(T_o - T_i)}{\eta_i I_T} \tag{4}$$

Where η_i is the energy efficiency of the collector, and it is calculated by this equation

$$\eta_i = \frac{\dot{m} C_p \,(T_o - T_i)}{A_c I_T} = \frac{A_c F_R [I_T\,(\tau\alpha) - U_L\,(T_i - T_a)]}{A_c I_T} \tag{5}$$

Another equation represents the energy efficiency of the collector that is used to obtain the efficiency curves from the experiments.

$$\eta_i = F_R(\tau\alpha) - F_R U_L \frac{(T_i - T_a)}{I_T} \tag{6}$$

3.2. Exergy calculations

This equation is used to calculate the exergy analysis as explained in Refs. [19–21].

$$\dot{E}x_{in} + \dot{E}x_{out} + \dot{E}x_{\,st} + \dot{E}x_{\,leak} + \dot{E}x_{dest} = 0 \tag{7}$$

Where $\dot{E}x_{in}$ represents the inlet exergy rate and it has two components, which are the solar energy absorbed ($\dot{E}x_{in,s}$) and the fluid flow ($\dot{E}x_{in,f}$) and they can be calculated by

$$\dot{E}x_{in,s} = I_T A_c \left(1 - \frac{T_a}{T_s}\right) \tag{8}$$

Table 2
Properties of MgO, MWCNT and water at 300K.

	C_P (J/Kg.K)	ρ (kg/m^3)	k(W/m.K)
MgO	877	3580	42
MWCNT	4180	2600	6150
Water	730	998	0.61

$$\dot{E}x_{in,f} = \dot{m}C_{p,NF}\left(T_i - T_a - T_a\ \ln\left({T_i}/{T_a}\right)\right) + \frac{\dot{m}\Delta P}{\rho} \tag{9}$$

Where ΔP represents the pressure drop and T_s represents the sun surface temperature. $\dot{E}x_{out}$ represents the outlet exergy rate, and it has a fluid flow component, and it can be calculated by

$$\dot{E}x_{out,f} = \dot{m}C_{p,NF}\left(T_o - T_a - T_a\ \ln\left({T_o}/{T_a}\right)\right) - \frac{\dot{m}\Delta P}{\rho} \tag{10}$$

$\dot{E}x_{dest}$ is the exergy destruction rate, and it can be calculated by

$$\dot{E}x_{dest} = T_a\dot{S}_{gen} \tag{11}$$

Where $\dot{S}_{gen}$ represents the overall entropy generation for ETSC and it is calculated by

$$\dot{S}_{gen} = \ \dot{m}C_{p,NF}\left(\ln\left({T_o}/{T_i}\right)\right) - \frac{q_{abs}}{T_s} + \frac{q_{loss}}{T_a} \tag{12}$$

Where q_{abs} represent the useful absorbed energy by the collector and q_{loss} is the lost energy by the collector to the environment, and it is calculated by

$$q_{loss}\ = q_{abs} - \dot{m}C_p(T_o\ -\ T_i) \tag{13}$$

The exergetic efficiency can be calculated by the following equation

$$\eta_{ex} = 1 - \frac{T_a\dot{S}_{gen}}{\left[1 - \left({T_a}/{T_s}\right)\right]q_{abs}} \tag{14}$$

3.3. Hybrid nanofluid properties calculations

The calculation of the density of the nanofluid and hybrid nanofluid is presented in Eq. (15) and Eq. (16) by Ref. [22,23].

$$\rho_{nf} = (1 -\ \varphi)\rho_{bf} + \varphi_{np} \tag{15}$$

$$\rho_{hnf} = \left(1 - \varphi_{np1} - \varphi_{np2}\right)\rho_{bf} + \varphi_{np1}\rho_{np1} + \varphi_{np2}\rho_{np2} \tag{16}$$

Where φ is the volume concentration. Ref. [22,23] provides heat capacity equations for nanofluids and hybrid nanofluids in Eqs. (17) and (18).

$$C_{p,nf} = \frac{\varphi\rho_{np}C_{p,np} + (1-\varphi)\rho_{bf}C_{p,bf}}{\rho_{nf}} \tag{17}$$

$$C_{p,hnf} = \frac{\varphi_{np1}\rho_{np1}C_{p,np1} + \varphi_{np2}\rho_{np2}C_{p,np2} + \left(1 - \varphi_{np1} - \varphi_{np2}\right)\rho_{bf}C_{p,bf}}{\rho_{hnf}} \tag{18}$$

The thermal properties of MgO, MWCNT and water are presented in Table 2.

3.4. Uncertainty analysis

The results of the experimental work are validated by the error assessment. The uncertainty analysis is calculated in Eq. (19).

$$U_y^2 = \sum_{i=1}^{n} U_{xi}^2 \tag{19}$$

Where U_y represents the total uncertainty parameter and U_{xi} represents the uncertainty for each parameter.

The total uncertainty of ETSC efficiency can be calculated in Eq. (20) in this present work where the main measured parameters are the mass flow rate (ṁ), solar intensity (I_T), inlet temperature (T_i), and outlet temperature (T_o). However, the collector area (A_c) and specific heat capacity (C_p) are assumed to have negligible errors.

Table 3
Uncertainty of measurement devices.

Parameter	Device	Uncertainty
Flow rate	Flow meter YF-S201	±1.6%
Inlet and outlet temperature	Thermocouple PT1000	±1.25%
Solar intensity	Solar Power Meter PYR 1307	±1.1%

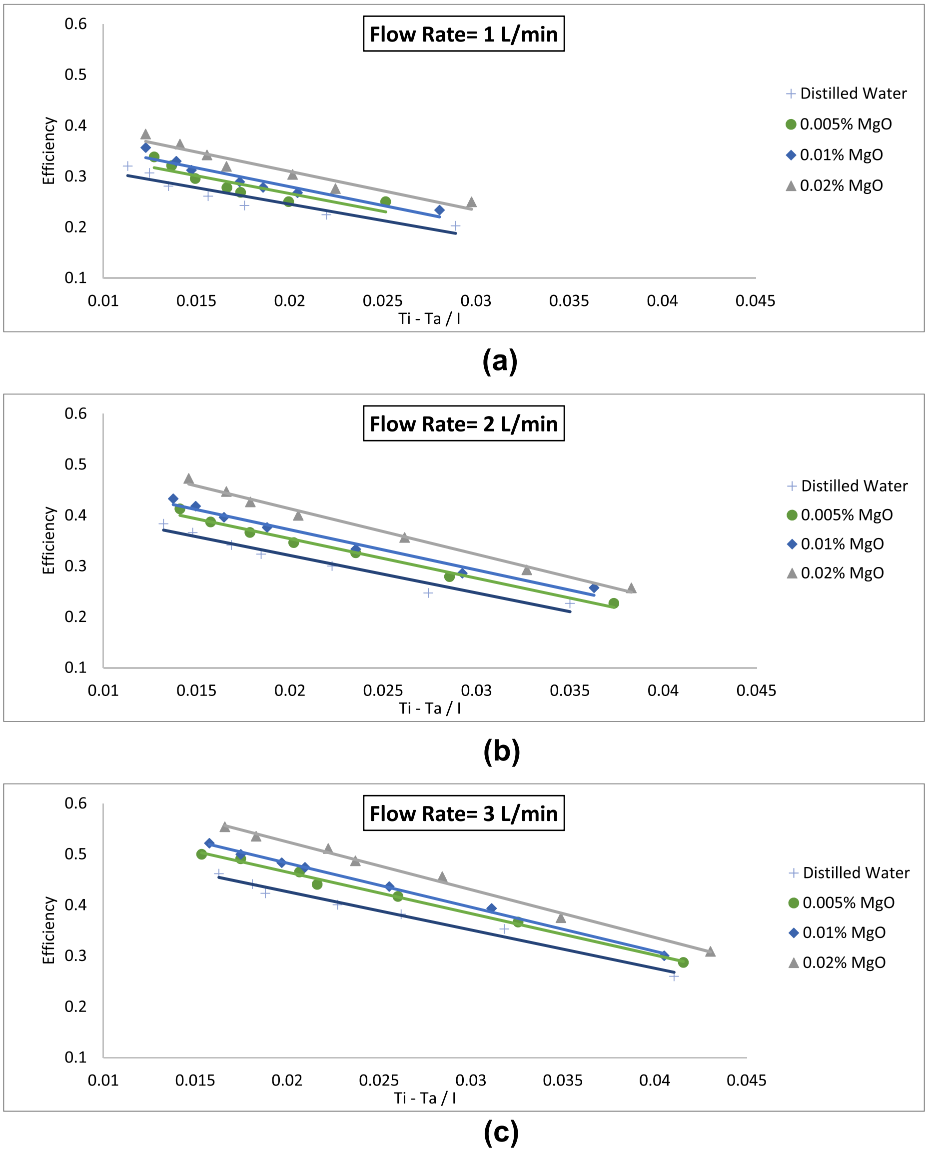

Fig. 2. Efficiency of the ETSC for MgO/water at different volume flow rates (a) 1L/min (b) 2L/min (c) 3L/min.

$$U_y = \eta_i \times \sqrt{\left(\frac{U_{\dot{m}}}{\dot{m}}\right)^2 + \left(\frac{U_{I_T}}{I_T}\right)^2 + \left(\frac{U_{T_{in}}}{T_{in}}\right)^2 + \left(\frac{U_{T_{out}}}{T_{out}}\right)^2} \qquad (20)$$

Where $U_{\dot{m}}$ represents the uncertainty of the mass flow rate. U_{I_T} represents the uncertainty of the solar intensity. The uncertainty of the inlet and outlet temperatures is represented by $U_{T_{in}}$. The total uncertainty for the efficiency of the collector is 2%, and the uncertainty for each parameter is presented in Table 3.

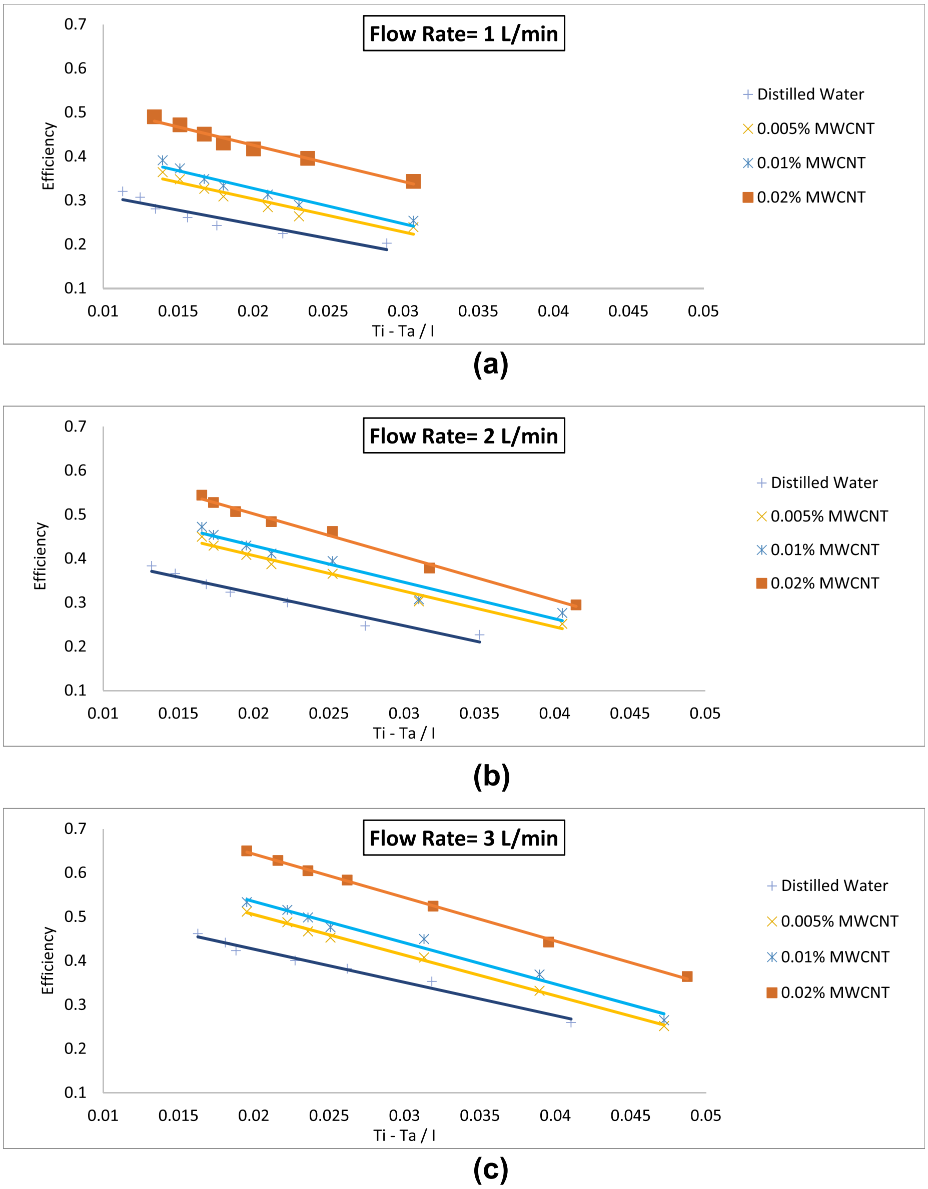

Fig. 3. Efficiency of the ETSC for MWCNT/water at different volume flow rates (a) 1L/min (b) 2L/min (c) 3L/min.

4. Results and discussions

In the present study, the energetic and exergetic efficiencies are used to investigate the thermal performance of the solar collector. In the first experiment, distilled water was tested as a working fluid to build a standard comparison with other working fluids. Three different particle concentrations were examined for MgO/water and MWCNT/water nanofluids at three different volume flow rates ranging from 1 to 3 L/min. A hybrid nanofluid of MgO/MWCNT in a water base was prepared and tested at four different weight ratios at the highest particle concentration.

4.1. *Thermal efficiency analysis using nanofluid with different concentrations*

The thermal efficiency is calculated based on Eq. (6) and it is plotted on the y-axis against the reduced temperature parameter $[(T_i - T_a)/I_T]$ on the x-axis where the measured points are fitted in a straight line to obtain the absorbed energy parameter $F_R(\tau\alpha)$, which represents the optical efficiency of ETSC, and the removal energy parameter $(F_R U_L)$, which is the slope of the straight line, and it represents the energy loss from the collector to the surroundings.

In this subsection, the thermal efficiency of ETSC is investigated using distilled water and three different concentrations of 0.005, 0.01 and 0.02% for MgO/water and MWCNT/water nanofluids. The thermal efficiencies of the collector for distilled water, MgO/water, and MWCNT/water are shown in Fig. 2 (a-c) and 3 (a-c), respectively. Increasing the volume flow rate enhances the thermal

Table 4
Observed values of $F_R(\tau\alpha)$ and $(F_R U_L)$ for MgO/water and MWCNT/water nanofluids.

Volume flow rate (L/min)	Weight fraction (%)	$F_R(\tau\alpha)$	$F_R U_L$
1	Distilled water	0.374	6.461
	0.005% MgO	0.406	7.005
	0.01% MgO	0.428	7.392
	0.02% MgO	0.462	7.625
	0.005%MWCNT	0.454	7.515
	0.01% MWCNT	0.488	8.049
	0.02% MWCNT	0.591	8.278
2	Distilled water	0.468	7.377
	0.005% MgO	0.51	7.795
	0.01% MgO	0.53	7.919
	0.02% MgO	0.592	8.973
	0.005%MWCNT	0.569	8.11
	0.01% MWCNT	0.595	8.305
	0.02% MWCNT	0.698	9.824
3	Distilled water	0.577	7.541
	0.005% MgO	0.628	8.165
	0.01% MgO	0.656	8.675
	0.02% MgO	0.713	9.412
	0.005%MWCNT	0.69	9.232
	0.01% MWCNT	0.723	9.384
	0.02% MWCNT	0.839	9.859

efficiency of the collector for all working fluids. The presence of the MgO and MWCNT nanoparticles improves the heat transfer of the working fluid. The highest thermal efficiency was observed at the highest volume flow rate and particle concentration for MWCNT/water nanofluid due to its higher thermal characteristics.

Table 4 presents the values of $F_R(\tau\alpha)$ and $(F_R U_L)$ for MgO/water and MWCNT/water nanofluids, respectively. It was observed that the augmentation of the volume flow rate and the particle concentration for MgO/water and MWCNT/water nanofluids increases the values of $F_R(\tau\alpha)$ and $(F_R U_L)$, respectively. The highest values of $F_R(\tau\alpha)$ were observed at 0.02% concentration for MgO/water and MWCNT/water at a volume flow rate of 3 L/min. Therefore, adding more nanoparticles will increase the efficiency of ETSC. The enhancement in the heat transfer is caused by Brownian motion, which is the random movement of the nanoparticles resulting in collisions with the base fluid. These collisions augment the transferred heat within the nanofluid.

The results proved that MWCNT/water nanofluid has the highest value of $F_R(\tau\alpha)$ compared to distilled water and MgO/water nanofluid at all particle concentrations and volume flow rates as it has the highest thermal conductivity. Hence, the heat energy gained by the working fluid is enhanced. On the other hand, $(F_R U_L)$ reached its highest value for MWCNT/water nanofluid at 0.02% concentration at a volume flow rate of 3 L/min. The main reason for this increase is that the augmentation in particle concentration will increase its sedimentation. Hence, the heat transfer of the working fluid will deteriorate quickly due to the rise in the viscosity value.

4.2. Thermal efficiency analysis using hybrid nanofluid

In this subsection, MgO/MWCNT hybrid nanofluid is tested at 0.02% concentration as it achieved the highest thermal performance of ETSC for both MgO/water and MWCNT/water nanofluids. The thermal efficiency of ETSC was investigated at three volume flow rates ranging from 1 to 3 L/min and four weight ratios of (80:20), (70:30), (60:40), and (50:50) for MgO/MWCNT hybrid nanofluids. Fig. 4 (a-c) shows the thermal efficiency of ETSC for distilled water, MgO/water, hybrid nanofluids of MgO/MWCNT (80:20), MgO/MWCNT (70:30), MgO/MWCNT (60:40), MgO/MWCNT (50:50) and MWCNT/water nanofluid with a particle concentration of 0.02% at volume flow rates of 1 L/min, 2 L/min, and 3 L/min, respectively. Table 5 presents the values of the absorbed energy parameter $F_R(\tau\alpha)$ and the removal energy parameter $(F_R U_L)$ for MgO/MWCNT hybrid nanofluids.

According to the results shown in Table 5 and Fig. 4 (a-c), increasing the volume flow rate and the weight ratios of MWCNTs nanoparticles improved the thermal performance of ETSC. The hybrid nanofluid of MgO/MWCNT (50:50) showed the best thermal performance compared to other hybrid nanofluids but is closer to MWCNT/water nanofluid. The reason for this result is that increasing the weight ratios of MWCNTs nanoparticles affects the thermal conductivity, density, and heat capacity of the working fluid. The mechanism of enhancing the thermal conductivity of hybrid nanofluids can be described as the dynamic motion of the particles that causes random collisions between the nanoparticles and the base fluid. Hence, micro-moments of nanoparticles will be generated, and this will enhance the thermal diffusion within the nanofluid. Another reason is the presence of the nanolayer, which is formed between solid nanoparticles and base fluid. This layer is responsible for transferring heat within the nanofluid. Nanoparticles have free electrons in their outer orbit, and they are responsible for increasing the heat transfer between the nanoparticles and base fluid. This enhancement improves the heat gain of the solar collector by intensifying the energy transport properties. The highest values of the average useful heat gain were observed at a volume flow rate of 3 L/min. The average useful heat gain by the collector had increased from 353 W for distilled water to 421 W, 433 W, 455 W, 471 W, 479 W, and 495 for MgO/water nanofluid, hybrid nanofluids of MgO/MWCNT (80:20), MgO/MWCNT (70:30), MgO/MWCNT (60:40), MgO/MWCNT (50:50), and MWCNT/water nanofluid, respectively.

The heat removal factor (F_R) is affected by the thermophysical properties of the working fluid. Accordingly, increasing the thermal conductivity of the working fluid enhances the heat removal factor (F_R). This enhancement increases the outlet temperature of the

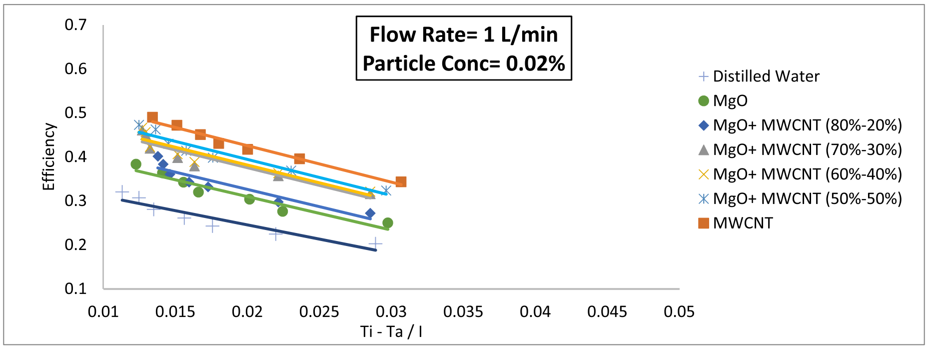

(a)

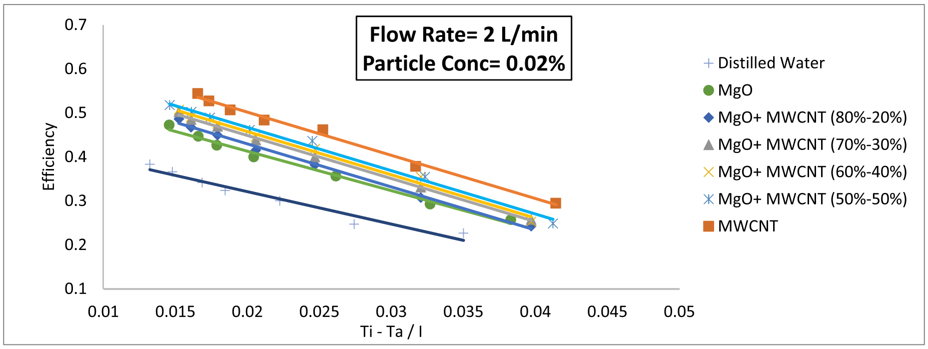

(b)

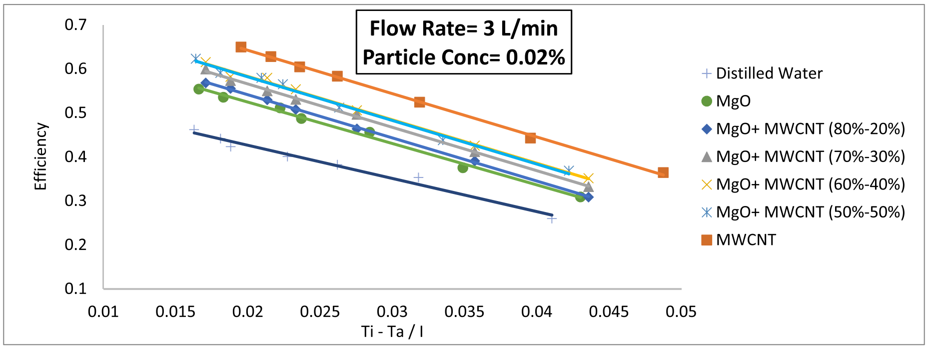

(c)

Fig. 4. Thermal efficiency of the ETSC for MgO/water, MWCNT/water and MgO/MWCNT hybrid nanofluids at different volume flow rates (a) 1L/min (b) 2L/min (c) 3L/min.

working fluid. However, it becomes less effective at higher volume flow rates. The reason for this phenomenon is that the inlet temperature of the fluid increases at higher volume flow rates, reducing the inlet-outlet temperature difference of the working fluid. On the other hand, the residence time to heat the working fluid is longer at lower volume flow rates. Therefore, the inlet-outlet temperature difference will rise. The augmentation of the outlet temperature of the working fluid in ETSC is influenced by the values of the heat capacity and effective density. The presence of MWCNTs nanoparticles reduces the heat capacity of the hybrid nanofluid, leading to higher outlet temperatures at a particular volume flow rate. A higher weight ratio of MWCNTs nanoparticles enhances the effective density of the hybrid nanofluid. This effect will augment the heat energy absorption from the absorber tube, and hence, the outlet temperature of the working fluid will be enhanced. The hybrid nanofluid of MgO/MWCNT (50:50) has lower heat capacity and higher effective density than other hybrid nanofluids. Therefore, a higher outlet temperature of the working fluid will be observed.

It was observed that increasing the weight ratios of MWCNT nanoparticles from 20% to 30% had a significant increase in the collector efficiency enhancement by 16.4% compared to other hybrid nanofluids at a volume flow rate of 1 L/min. However, this enhancement has decreased at higher volume flow rates. The explanation for this effect is that increasing the inlet temperature of the working fluid will raise the values of the reduced temperature parameter $[(T_i - T_a)/I_T]$, resulting in higher convection losses. The highest thermal collector efficiency enhancements recorded are 21.67%, 29.65%, 50.95%, 53.61%, 55.89%, and 62.73%, respectively,

Table 5
Observed values of $F_R(\tau\alpha)$ and $(F_R U_L)$ for MgO/water, MWCNT/Water and MgO/MWCNT hybrid nanofluids at 0.02% particle concentration.

Volume flow rate (L/min)	Working fluid	$F_R(\tau\alpha)$	$F_R U_L$
1	Distilled water	0.374	6.461
	MgO/water	0.406	7.005
	MgO/MWCNT (80:20)	0.483	7.848
	MgO/MWCNT (70:30)	0.536	8.046
	MgO/MWCNT (60:40)	0.543	8.068
	MgO/MWCNT (50:50)	0.558	8.187
	MWCNT/water	0.591	8.278
2	Distilled water	0.468	7.377
	MgO/water	0.51	7.795
	MgO/MWCNT (80:20)	0.625	9.786
	MgO/MWCNT (70:30)	0.644	9.792
	MgO/MWCNT (60:40)	0.654	9.841
	MgO/MWCNT (50:50)	0.664	9.846
	MWCNT/water	0.698	9.824
3	Distilled water	0.577	7.541
	MgO/water	0.628	8.165
	MgO/MWCNT (80:20)	0.737	9.81
	MgO/MWCNT (70:30)	0.763	9.854
	MgO/MWCNT (60:40)	0.78	9.87
	MgO/MWCNT (50:50)	0.781	9.918
	MWCNT/water	0.839	9.859

for MgO/water, hybrid nanofluids of MgO/MWCNT (80:20), MgO/MWCNT (70:30), MgO/MWCNT (60:40), MgO/MWCNT (50:50), and MWCNT/water at a volume flow rate of 1 L/min. It can be deduced that the highest value of $F_R(\tau\alpha)$ was 0.839 for MWCNT/water nanofluid at a volume flow rate of 3 L/min. However, the highest value of $(F_R U_L)$ was 9.918 for MgO/MWCNT (50:50) at the same volume flow rate. The results showed that MgO/MWCNT (80:20) hybrid nanofluid had obtained the lowest thermal performance compared to other hybrid nanofluids, but it performed better than MgO/water nanofluid.

4.3. Exergy analysis

The thermal efficiency of ETSC is affected by the irreversibility losses. It is essential to investigate the exergetic performance of ETSC to evaluate the maximum available energy that can be converted to useful heat. Exergy destruction, entropy generation, and exergy efficiency were investigated for MgO/MWCNT hybrid nanofluids at mass flow rates of 0.0167 kg/s, 0.033 kg/s, and 0.05 kg/s. Fig. 5 (a-c) shows the exergy destruction, entropy generation, and exergy efficiency against the mass flow rate for distilled water, MgO/water nanofluid, hybrid nanofluids of MgO/MWCNT (80:20), MgO/MWCNT (70:30), MgO/MWCNT (60:40), MgO/MWCNT (50:50), and MWCNT/water nanofluid. It can be deduced that MgO/MWCNT hybrid nanofluids have reduced the exergy destruction significantly with the addition of the MWCNT nanoparticles. Accordingly, MgO/MWCNT (50:50) has a higher reduction in exergy destruction compared to distilled water, MgO/water, and other hybrid nanofluids, but slightly less than MWCNT/water nanofluid. However, the exergy destruction has increased for all working fluids at higher flow rates.

It was observed that distilled water had the highest entropy generation compared to other working fluids at all flow rates. Due to its high thermal conductivity, MWCNT/water nanofluid had the highest reduction in entropy generation. The reason for this effect is that the heat transfer between the heat pipe and the working fluid by conduction was improved. Moreover, adding MWCNT nanoparticles increases the viscosity of the working fluid, affecting the entropy generation. The heat transfer and mass flow rates of the ETSC affect the values of the entropy generation. It can be observed that the values of the entropy generation were lower at a low mass flow rate as the friction value and pressure drop were less significant. However, at a higher mass flow rate, the values of the entropy generation increase significantly, reducing the mean temperature value of the ETSC. It is not recommended to have higher entropy generation as it reveals that the system has a lower capability to convert the available energy into useful energy. The exergy efficiency was enhanced with the increase of the mass flow rate and by adding MWCNT nanoparticles. For a flow rate of 1 L/min, the highest enhancement of the exergy efficiency is 33.55%, 44%, 64.51%, 67.44%, 77.14%, and 88.12% MgO/water nanofluid, hybrid nanofluids of MgO/MWCNT (80:20), MgO/MWCNT (70:30), MgO/MWCNT (60:40), MgO/MWCNT (50:50), and MWCNT/water nanofluid, respectively. It can be concluded that MgO/MWCNT (50:50) hybrid nanofluid has improved exergy efficiency higher than other hybrid nanofluids but slightly less than the MWCNT/water nanofluid.

5. Conclusion

The energetic and exergetic efficiencies of the evacuated tube solar collector were experimentally investigated using MgO/MWCNT hybrid nanofluid for a particle concentration of 0.02% at three volume flow rates ranging from 1 to 3 L/min and four weight ratios of (80:20), (70:30), (60:40), and (50:50). The main findings of this research are highlighted as follows:

- The energy and exergy efficiencies of the ETSC were improved by increasing the volume flow rate and the weight ratio of MWCNT nanoparticles, respectively.

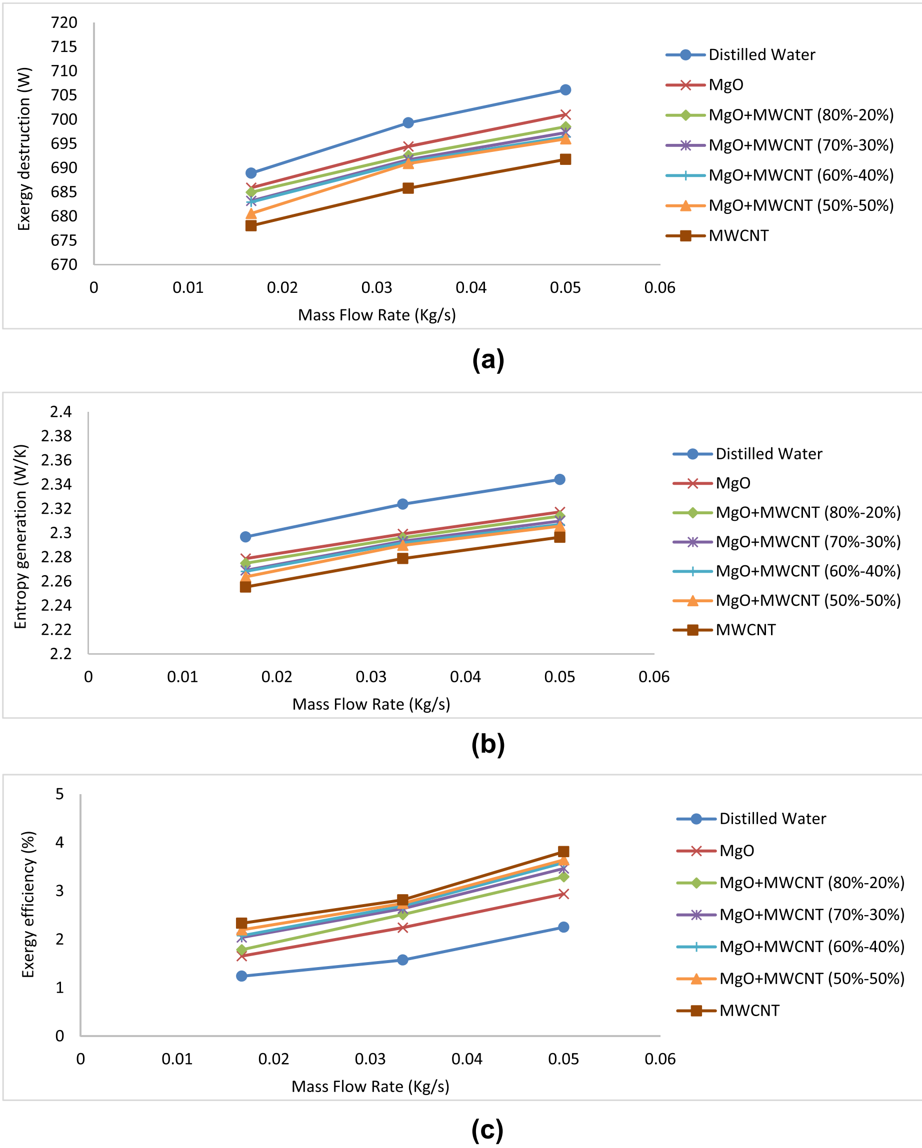

Fig. 5. Different mass flow rates and weight ratios of MgO/MWCNT hybrid nanofluid versus (a) Exergy destruction (b) Entropy generation (c) Exergy efficiency.

- It can be deduced that MgO/MWCNT (50:50) hybrid nanofluid had achieved the highest thermal performance compared to hybrid nanofluids of MgO/MWCNT (70:30), MgO/MWCNT (60:40), and MgO/MWCNT (50:50) at all volume flow rates, but it was slightly lower than MWCNT/water nanofluid.
- The results showed that MgO/MWCNT (80:20) hybrid nanofluid had obtained the lowest thermal performance compared to other hybrid nanofluids at all volume flow rates, but it performed better than MgO/water nanofluid.
- It was observed that changing the working fluid from MgO/MWCNT (80:20) to MgO/MWCNT (70:30) had attained a significant increase in the collector efficiency enhancement compared to other hybrid nanofluids.
- The highest values of the absorbed energy parameter represented as $F_R(\tau\alpha)$ and the removal energy parameter represented as $(F_R U_L)$ were achieved by MWCNT/water nanofluid for a particle concentration of 0.02% at all volume flow rates. However, at a volume flow rate of 2 L/min and 3 L/min, the values of $(F_R U_L)$ for MgO/MWCNT (50:50) hybrid nanofluid were slightly higher.
- The highest value of $F_R(\tau\alpha)$ was 0.839 for MWCNT/water nanofluid at a volume flow rate of 3 L/min. On the other hand, the highest value of $(F_R U_L)$ was 9.918 for MgO/MWCNT (50:50) hybrid nanofluid in the same case.
- At a volume flow rate of 1 L/min, MWCNT/water nanofluid had achieved the highest exergy efficiency enhancement of 88.12%, followed by 77.14% for MgO/MWCNT (50:50) hybrid nanofluid.
- It can be concluded that MgO/MWCNT hybrid nanofluid significantly reduced the entropy generation and exergy destruction of the ETSC compared to distilled water.

- It can be considered that MgO/MWCNT hybrid nanofluid is a potential alternative working fluid to MWCNT/water nanofluid that offers better thermal and rheological properties and a lower cost of the raw material.
- Investigating different weight ratios of hybrid nanofluid opens a field of research to explore cost-effective working fluids in solar collectors.

Declaration of competing interest

The authors declare that they have no known competing financial interests or personal relationships that could have appeared to influence the work reported in this paper.

Acknowledgement

Our sincere thanks to the Centre for Renewable Energy (CRE) at The British University in Egypt for providing the experimental apparatus to carry out the research in the renewable energy laboratory.

References

[1] M. Eltaweel, A. Abdel-Rehim, A comparison between flat-plate and evacuted tube solar collector in terms of energy and exergy analysis by using nanofluid, Appl. Therm. Eng. 186 (2021) 116516.
[2] S. Delfani, M. Karami, M. Behabadi, Performance characteristics of a residential-type direct absorption solar collector using MWCNT nanofluid, Renew. Energy 87 (2016) 754–764.
[3] P. Martínez-Merino, R. Alcántara, P. Gómez-Larrán, I. Carrillo-Berdugo, J. Navas, MoS2-based nanofluids as heat transfer fluid in parabolic trough collector technology, Renew. Energy 188 (2022) 721–730.
[4] S. Rashidi, S. Akar, M. Bovand, R. Ellahi, Volume of fluid model to simulate the nanofluid flow and entropy generation in a single slope solar still, Renew. Energy 115 (2018) 400–410.
[5] A. Noghrehabadi, E. Hajidavalloo, M. Moravej, Experimental investigation of efficiency of square flat-plate solar collector using SiO2/water nanofluid, Case Stud. Therm. Eng. 8 (2016) 378–386.
[6] H. Kaya, M. Alkasem, K. Arslan, Effect of nanoparticle shape of Al2O3/Pure Water nanofluid on evacuated U-Tube solar collector efficiency, Renew. Energy 162 (2020) 267–284.
[7] S. Gupta, S. Gupta, The role of nanofluids in solar thermal energy: a review of recent advances, Mater. Today Proc. 44 (2021) 401–412.
[8] R. Pankaj, S. Sudhakar, A review of studies using nanofluids in flat-plate and direct absorption solar collectors, Renew. Sustain. Energy Rev. 84 (2018) 54–74.
[9] M. Sharafeldin, G. Gróf, E. Abu-Nada, O. Mahian, Evacuated tube solar collector performance using copper nanofluid: energy and environmental analysis, Appl. Therm. Eng. 162 (2019) 114205.
[10] M. Eltaweel, A. Abdel-Rehim, A. Attia, Energetic and exergetic analysis of a heat pipe evacuated tube solar collector using MWCNT/water nanofluid, Case Stud. Therm. Eng. 22 (2020) 100743.
[11] M. Eltaweel, A. Abdel-Rehim, Energy and exergy analysis for stationary solar collectors using nanofluids: a review, Int. J. Energy Res. (2020) 1–28.
[12] H. Babar, H. Ali, Towards hybrid nanofluids: preparation, thermophysical properties, applications, and challenges, J. Mol. Liq. 281 (2019) 598–633.
[13] T. Hayat, S. Nadeem, Heat transfer enhancement with Ag–CuO/water hybrid nanofluid, Results Phys. 7 (2017) 2317–2324.
[14] M. Esfe, A. Alirezaie, M. Rejvani, An applicable study on the thermal conductivity of SWCNT-MgO hybrid nanofluid and price-performance analysis for energy management, Appl. Therm. Eng. 111 (2017) 1202–1210.
[15] F. Sani, M. Pourfallah, M. Gholinia, The effect of MoS2–Ag/H2O hybrid nanofluid on improving the performance of a solar collector by placing wavy strips in the absorber tube, Case Stud. Therm. Eng. 30 (2022) 101760.
[16] E. Yıldırım, A. Yurddas, Assessments of thermal performance of hybrid and mono nanofluid U-tube solar collector system, Renew. Energy 171 (2021) 1079–1096.
[17] M. Abid, M. Khan, T. Ratlamwala, M. Malik, H. Ali, Q. Cheok, Thermodynamic analysis and comparison of different absorption cycles driven by evacuated tube solar collector utilizing hybrid nanofluids, Energy Convers. Manag. 246 (2021) 114673.
[18] S. Verma, A. Tiwari, S. Tiwari, D. Chauhan, Performance analysis of hybrid nanofluids in flat plate solar collector as an advanced working fluid, Sol. Energy 167 (2018) 231–241.
[19] S. Kalogirou, Solar Energy Engineering, vol. 2, Elsevier/Academic Press, Burlington, MA, 2009.
[20] S. Farahat, F. Sarhaddi, H. Ajam, Exergetic optimization of flat plate solar collectors, Renew. Energy 34 (4) (2009) 1169–1174.
[21] A. Alanazi, Y. Khetib, H. Abo-Dief, M. Rawa, G. Cheraghian, M. Sharifpur, The effect of nanoparticle shape on alumina/EG-water (50:50) nanofluids flow within a solar collector: entropy and exergy investigation, Case Stud. Therm. Eng. 28 (2021) 101510.
[22] B. Pak, I. Young, Hydrodynamic and heat transfer study of dispersed fluids with submicron metallic oxide particles, Exp. Heat Tran. 11 (2007) 151–170.
[23] B. Takabi, S. Salehi, Augmentation of the heat transfer performance of a sinusoidal corrugated enclosure by employing hybrid nanofluid, Adv. Mech. Eng. (2014).